Journal of Nuclear Materials 424 (2012) 51–56

Contents lists available at SciVerse ScienceDirect

Journal of Nuclear Materials

journal homepage: www.elsevier.com/locate/jnucmat

Adsorption and dissociation of H_2O on Zr(0001) with density-functional theory studies

Shuang-Xi Wang [a,b,c,1], Ping Zhang [c,*], Peng Zhang [d], Jian Zhao [e], Shu-Shen Li [a]

[a] State Key Laboratory for Superlattices and Microstructures, Institute of Semiconductors, Chinese Academy of Sciences, P.O. Box 912, Beijing 100083, People's Republic of China
[b] Department of Physics, Tsinghua University, Beijing 100084, People's Republic of China
[c] LCP, Institute of Applied Physics and Computational Mathematics, P.O. Box 8009, Beijing 100088, People's Republic of China
[d] Department of Nuclear Science and Technology, Xi'an Jiaotong University, Xi'an 710049, People's Republic of China
[e] State Key Laboratory for Geomechanics and Deep Underground Engineering, China University of Mining and Technology, Beijing 100083, People's Republic of China

ARTICLE INFO

Article history:
Received 28 October 2011
Accepted 8 February 2012
Available online 18 February 2012

ABSTRACT

The adsorption and dissociation of isolated H_2O molecule on Zr(0001) surface are investigated by using density-functional theory calculations. It is shown that the flat adsorption states on the top site are dominated by the $1b_1$–d band coupling, insensitive to the azimuthal orientation. The diffusion between adjacent top sites reveals that the water molecule is very mobile on the surface. For the upright adsorption configuration on the bridge site, the surface → water charge transfer occurring across the Fermi level plays an important role. The dissociation of H_2O on Zr(0001) surface is very facile, in good accordance with the attainable experimental results.

1. Introduction

The adsorption of water on metal surfaces is of fundamental importance and has gained a lot of interest associated with a variety of phenomena such as heterogeneous catalysis and corrosion of materials [1,2]. As a result these systems have been intensively investigated by various experimental and theoretical techniques, especially for the transition metal surfaces, such as Cu(100) [3,4], Fe(100) [5,6], and Pd(100) [7,8]. From a practical point of view, it is critical to understand the bonding and orientation characteristics of water molecule on the surfaces. Experimentally, complicated by the facile H_2O cluster formation, it is difficult to discriminate between H_2O monomers and clusters. Thus ambiguities have arisen about the preferred orientation of H_2O molecule on the surfaces.

Theoretically an upright configuration has been proposed for the adsorption of water on metal surfaces [9,10]. It has been demonstrated that by maximizing the adsorbate-dipole substrate-image-dipole interactions, an upright H_2O favors interaction with the metal surfaces through the molecular orbitals (MOs) of water, mainly $3a_1$ orbital. Nevertheless, in later density-functional theory (DFT) calculations, a flat-lying configuration on the top site of transition metal surfaces has been established by some sophisticated studies [11–13], arguing that the $1b_1$ orbital dominates the water–surface interaction, by coupling with atomic d orbital of the transition metal surfaces. It is desirable to understand these conflicting results. Therefore, further systematic studies in this area are needed to obtain a thorough understanding of the water structure on metal surfaces.

In this paper, based on first-principles calculations, we investigate the adsorption properties of H_2O on Zr(0001) surface. Zirconium and its alloys have long been used in nuclear reactors as low neutron adsorption cross-section and excellent corrosion resistance [14]. Water is the main residual gas in the ultrahigh vacuum (UHV) vessels of the nuclear reactors, so it is highly meaningful to study the adsorption of water molecule at zirconium surfaces. The experimental investigations for the adsorption of water on Zr(0001) have been done with various techniques, including low-energy electron diffraction (LEED) [15,16] and photoemission spectroscopy [17]. Water was found to adsorb on the surface and autocatalytic decomposition took place, as a function of temperature (T) (170 K < T < 573 K). Despite the experimental results a detailed investigation on the electronic nature of water adsorption and dissociation on the Zr(0001) surface is indispensable to a complete understanding of water–metal interactions. Moreover, we expect that the present work helps to resolve current existing controversy mentioned above.

By detailed geometric optimizations and analysis of the electronic structures including the projected density of states (PDOS) and charge density difference, we obtain the adsorption properties of H_2O on Zr(0001) surface. The electronic structures of the stable adsorption states, as well as the diffusion and dissociation

* Corresponding author. Tel.: +86 10 62014411 2208; fax: +86 10 62014411 2958.
E-mail addresses: sxwang@semi.ac.cn (S.-X. Wang), zhang_ping@iapcm.ac.cn (P. Zhang).
[1] Tel.: +86 1062014411 2209; fax: +86 1062792457.

0022-3115/$ - see front matter © 2012 Elsevier B.V. All rights reserved.
doi:10.1016/j.jnucmat.2012.02.007

properties of the system are calculated and discussed in details, with the results compared with the attainable experimental measurements.

2. Computational methods

The calculations are performed using the DFT, as implemented in the Vienna *ab initio* simulation package (VASP) [18]. The PBE [19] generalized gradient approximation and the projector-augmented wave potential [20] are employed to describe the exchange–correlation energy and the electron–ion interaction, respectively. To assure the accurate results a cutoff energy of 400 eV for the plane wave expansion are used. The Zr(0001) surface is modeled by a slab composing of five atomic layers and a vacuum region of 20 Å. A 2×2 supercell, in which each monolayer contains four Zr atoms, is adopted in the study of the H_2O adsorption. The water molecule is placed on one side of the slab only and a dipole correction [21] is applied to compensate for the induced dipole moment. During our calculations, the bottom two atomic layers of the Zr substrate are fixed, and other Zr atoms as well as the H_2O molecule are free to relax until the forces on the ions are less than 0.02 eV/Å. Integration over the Brillouin zone is done using the Monkhorst–Pack scheme [22] with $7 \times 7 \times 1$ grid points. And a Fermi broadening [23] of 0.1 eV is chosen to smear the occupation of the bands around the Fermi level by a finite-T Fermi function and extrapolating to $T = 0$ K. In a previous publication we have already employed the present approach to study the adsorption of water on Be(0001) surface [24].

The energy barriers for the water diffusion and dissociation processes are calculated by using the nudged elastic band (NEB) method [25], which is a method for calculating the minimum energy path between two known minimum energy sites, by introducing a number of "images" along the diffusion path. Within each path the energy barrier is determined by relaxing the atomic positions of each image in the direction perpendicular to the path connecting the images, until a force convergence is achieved. In the present work, the diffusion path is modeled using seven images, two of which include the minimum energy sites as initial and final positions. As an initial guess, five linearly interpolated, intermediate images between the initial and final configuration are used.

3. Results and discussion

3.1. Adsorption properties

For free water molecule, the structural and energetic parameters are calculated within a box with the same size of the adsorbed systems. The optimized geometry for free H_2O gives a bond length of 0.97 Å and a bond angle of 104.2°, which agree well with the experimental values of 0.96 Å and 104.4° [26]. The calculated lattice constant of bulk Zr(a, c) are 3.24 Å and 5.18 Å, respectively, in good agreement with the experimental measurements of 3.233 Å and 5.146 Å [27].

As depicted in Fig. 1a, we consider four high-symmetry sites on the Zr(0001) surface, respectively the top, bridge (bri), hcp and fcc hollow sites. The O atom of water is initially placed on the precise high-symmetry sites with various orientations of water with respect to the substrate. We find that there exist locally stable adsorption states on the top site of Zr(0001), where the H_2O molecules lie fairly flat on the surface, labeled by employing the notations top-x, $y1$ and $y2$, respectively. Besides, our calculations demonstrate that the upright molecular configuration adsorbed on the bridge site with the O atom lying down is also a locally state molecular state, labeled by bri-z. The structural and energetic details of the molecular states are illustrated in Fig. 1b–e and summarized in Table 1. In Fig. 1b we define two angles ϕ and θ. ϕ represents the azimuthal angle of H_2O with respect to the surface, and θ represents the tilt angle between the H_2O molecular dipole plane and the surface. The adsorption energy of the system is calculated as follows:

$$E_{ad} = E_{H_2O/Zr(0001)} - E_{H_2O} - E_{Zr(0001)}, \quad (1)$$

where E_{H_2O}, $E_{Zr(0001)}$, and $E_{H_2O/Zr(0001)}$ are the total energies of the H_2O molecule, the clean Zr surface, and the adsorption system respectively. According to this definition, a negative value of E_{ad} indicates that the adsorption is exothermic (stable) with respect to a free H_2O molecule and a positive value indicates endothermic (unstable) reaction.

From Table 1, we can clearly see that at these stable adsorption sites, the work functions are much smaller than the clean Zr(0001) surface (4.26 eV), implying an observable charge redistribution between the adsorbate water and the surface Zr atoms. Taking the adsorption site top-$y1$ for example, the O–H bond length 0.99 Å is almost identical to 0.97 Å of free H_2O molecule, but the H–O–H bond angle 106.2° is larger than that of free H_2O. The tilt angle is 14.9°, differing a little from that (~10°) of other transition metal surfaces mentioned above, where the top site is the most stable state. The adsorption energy −0.616 eV indicates a stronger molecule-surface interaction than on other transition metal surfaces (usually of −0.3 eV). For the adsorption site bri-z, a lower work function 2.94 eV and a larger H–O–H bond angle 110.6° are identified, suggesting more prominent charge redistribution and molecular distortion compared to the top-site adsorption. It is clear that the bri-z adsorption almost has the same adsorption energy as the top-site adsorption. This is quite different from previous DFT calculations on other transition metal surfaces that predicted the flat-lying top-site adsorption to be the most stable configuration. Interestingly, for a H_2O molecule to reach the adsorption state, there does not exist any energy barrier, which means that H_2O can be adsorbed on the Zr(0001) surface directly.

As presented in Table 1, the energetic differences among these three adsorption states on top site are very tiny. For further illustration, we investigate the azimuthal orientation of the adsorbed H_2O, which is shown in Fig. 2. It can be seen that the adsorption site top-$y1$ is slightly more stable. Nevertheless, it is noted that the variation of the adsorption energy for different azimuthal orientations are determined to be less than 0.01 eV. We will see below that this is much smaller than the energy barrier of the lateral diffusion, implying that the azimuthal rotation is essentially unhindered and may occur at very low temperature.

In order to further understand the precise nature of the chemisorbed molecular state, the electronic PDOS of the H_2O molecule and the topmost Zr layer are calculated. As typical examples, here we plot in Fig. 3 the PDOS for the stable adsorption configurations of top-$y1$ and bri-z. For comparison, the PDOS of the free H_2O molecule and clean Zr(0001) surface are also shown in Fig. 3a. The three-dimensional (3D) electron density difference $\Delta\rho(\mathbf{r})$, which is obtained by subtracting the electron densities of noninteracting component systems, $\rho^{Zr(0001)}(\mathbf{r}) + \rho^{H_2O}(\mathbf{r})$, from the density $\rho(\mathbf{r})$ of the H_2O/Zr(0001) surface, while retaining the atomic positions of the component systems at the same location as in H_2O/Zr(0001), is also shown in the insets of Fig. 3. Positive (blue) $\Delta\rho(\mathbf{r})$ indicates accumulation of electron density upon binding, while a negative (yellow) one corresponds to electron density depletion. MO $2a_1$ of water (not shown here) is far below the Fermi level and thus remains intact in water–metal interaction. Here we consider only three MOs $1b_2$, $3a_1$, and $1b_1$.

In the case of adsorption on the top-$y1$ site, as illustrated in Fig. 3b, these three MOs are rigidly shifted downward by 1.57, 2.02 and 2.33 eV, respectively. This is essentially caused by the different electronegativities of Zr and water molecule, which induces

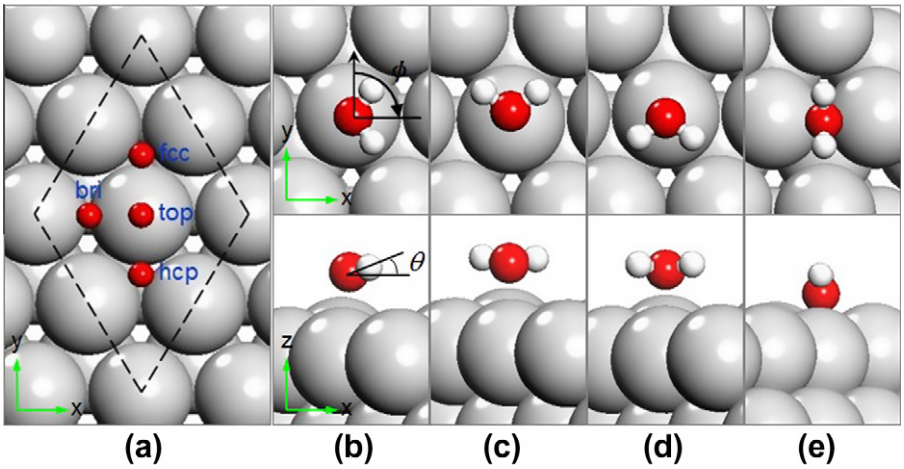

Fig. 1. (a) The structure of the p (2 × 2) surface cell of Zr(0001), and four on-surface adsorption sites, meanwhile the red balls denote the initial positions of O atoms in the adsorption picture. (b–e) Top view (upper panels) and side view (lower panels) of the optimized structures of four most stable adsorption states of H_2O/Zr(0001) surface, i.e., top-*x*, top-*y*1, top-*y*2, and bri-*z*, respectively. Gray, red and white balls denote Zr, O, and H atoms, respectively. (For interpretation of the references to colour in this figure legend, the reader is referred to the web version of this article.)

Table 1
Calculated structural parameters, adsorption energy for a water molecule on Zr(0001) surface. E_a (eV) represents the adsorption energy. Φ (eV) represents the work function. z_O (Å) represents the vertical height of the O atom from the surface, the height of which is averaged over all atoms on the surface. d_{O-H} (Å) represents the bond length between the O and H atoms. θ (°) represents the tilt angle between the H_2O molecular dipole plane and the surface. α (°) represents the H–O–H bond angle.

Site	E_a	Φ	z_O	d_{O-H}	θ	α
top-*x*	−0.611	3.35	2.35	0.99	16.8	105.9
top-*y*1	−0.616	3.38	2.35	0.99	14.9	106.2
top-*y*2	−0.609	3.35	2.34	0.99	15.9	106.1
bri-*z*	−0.610	2.94	1.88	0.99	90.0	110.6

charge redistribution and thus build a global electrostatic attraction between the water and substrate. In addition to this rigid energy shift, it is also noticeable that due to the molecule–metal orbital hybridization, the MOs of adsorbed water are broadened apparently for $1b_1$ and $3a_1$, which are known to have an oxygen lone-pair character perpendicular to the molecular plane, and a mixture of partial lone-pair character parallel to the molecular plane and partial O–H bonding character, respectively [1,6]. Remarkably, the water adsorption introduces new peaks for both d_{z^2} and d_{yz} states of the surface Zr atom, aligning in energy with $1b_1$ and $3a_1$. Especially for $1b_1$, more electronic states of the Zr atom, mostly d_{z^2} appear nearby, indicating that the adsorbed $1b_1$ MO may act as an electron donor state. This is quite in accordance with the general picture that the water–surface interaction is dominated by the $1b_1$–*d* band coupling. It is obvious that this kind of coupling cannot be effected essentially by the azimuthal rotation of the water, hence the adsorption of H_2O on the top site is insensitive to the azimuthal orientation. The features of the orbital hybridization are further substantiated by the 3D electron density difference plotted in the inset of Fig. 3b, from which we can see that there exists a large charge accumulation between the adsorbate and substrate.

For upright adsorption site bri-*z* (Fig. 3c), it is known that $3a_1$ plays an additional key role in the upright adsorption structure of water monomer [11]. Here obviously, the orbital $3a_1$ undergoes a noticeable broadening as well as $1b_1$. We notice that instead of d_{yz}, it is the state d_{xz} of the Zr atom, together with d_{z^2}, that overlaps with the orbital $1b_1$ of water. And new peaks for d_{xz} and d_{x^2} emerge aligning in energy with the orbital $3a_1$. This observable overlapping can also be seen from the 3D electron density difference plotted in the inset of Fig. 3c, from which we find a large charge accumulation

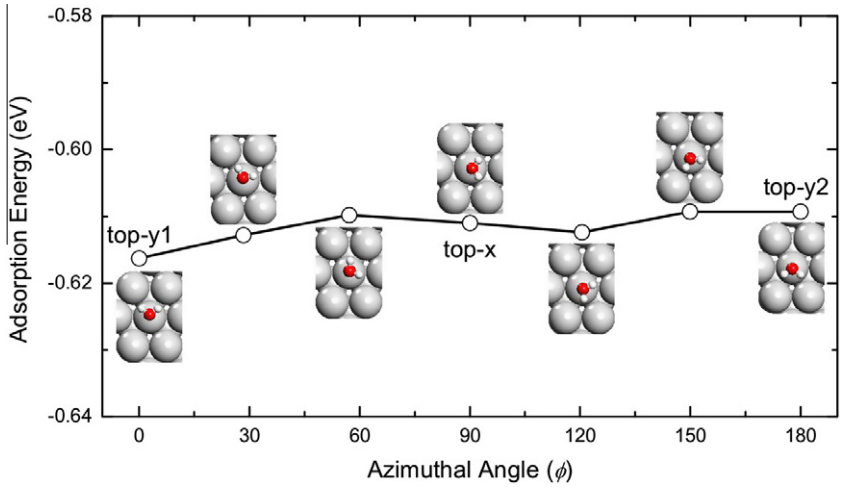

Fig. 2. Calculated adsorption energy of H_2O as a function of the azimuthal angle at the top site. The insets show the structures adopted in the calculations.

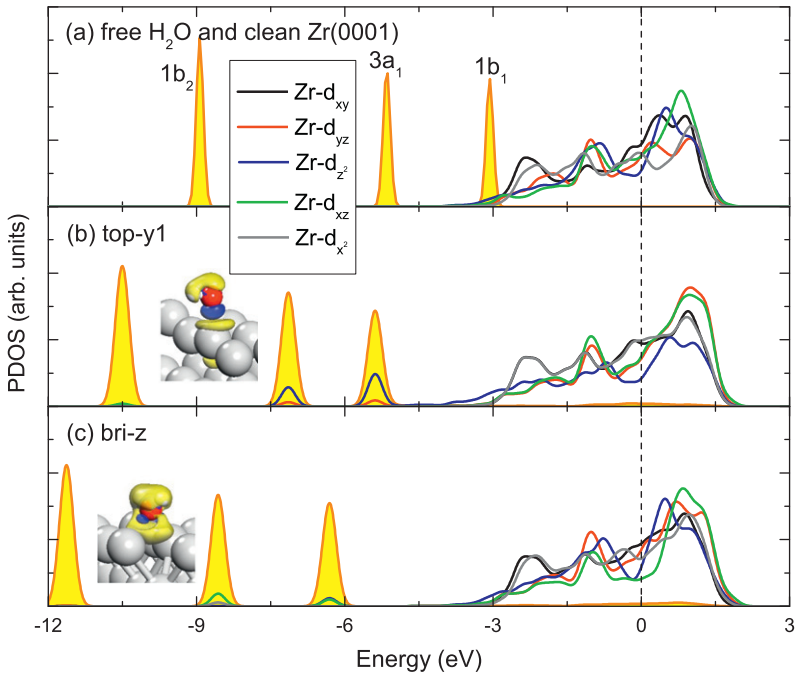

Fig. 3. The PDOS of the H_2O molecule and the top-layer Zr atom bonded to H_2O for (a) free H_2O and the clean Zr(0001) surface, (b) top-$y1$ adsorption site and (c) bri-z adsorption site. The insets in (b) and (c) show the 3D electron density difference, with the isosurface value set at ±0.015 $e/Å^3$. The area filled with yellow color represents molecular orbital of H_2O. The Fermi level is set to zero. (For interpretation of the references to color in this figure legend, the reader is referred to the web version of this article.)

between the O atom and two adjacent top-layer Zr atoms. Moreover, it is noteworthy that a discernible occupied domain of states of the adsorbed water emerges near the Fermi level, suggesting more prominent charge transfer between adsorbate and substrate than the top-site adsorption. We find that the emerged occupied state aligns with the lowest unoccupied MO, which coincides with the so-called Blyholder model [28], where an electron donation from the adsorbate highest occupied MO to substrate states and a back-donation from such states to the lowest unoccupied MO of the adsorbate build up the chemisorption bond. With a distortion of the adsorbed water, the MOs are shifted down by 2.70, 3.43 and 3.25 eV for $1b_2$, $3a_1$ and $1b_1$, respectively, which are more pronounced compared with those on top-$y1$, especially for the orbital $3a_1$, hence more unoccupied MOs are drawn below the Fermi level. Therefore, although observable is the overlapping, charge transfer is more prominent for the bri-z adsorption, leading to a considerable stable electrostatic bonding between water and the surface.

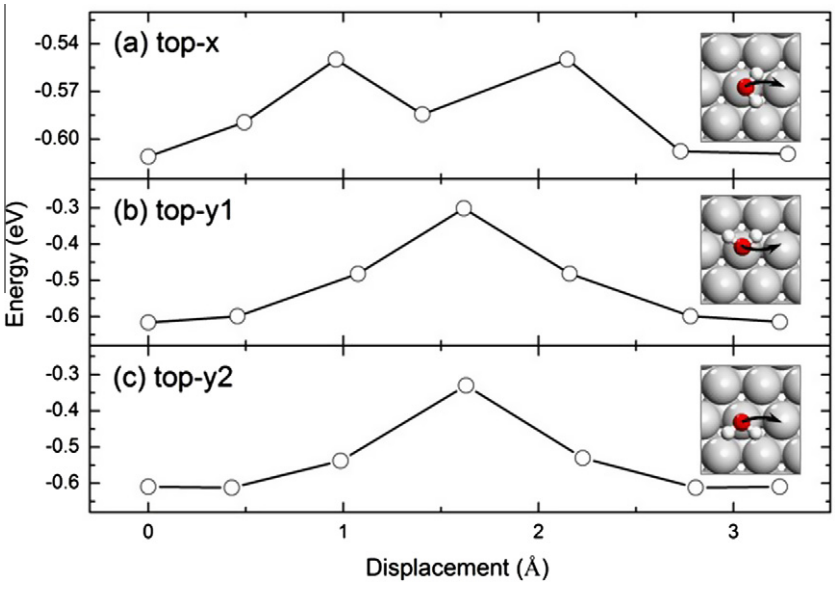

Fig. 4. Diffusion of H_2O on the top site of Zr(0001) surface as a function of the lateral displacement of O atom from its original site top-x (upper panel), top-$y1$ (middle panel), and top-$y2$ (lower panel), respectively.

Table 2
Calculated structural parameters, adsorption energy for water dissociation products on Zr(0001) surface. E_a (eV) represents the adsorption energy. z (Å) represents the vertical height of the H atom (for H species) or O atom (for OH species) from the surface.

Species	Site	E_a	z	d_{O-H}
H	hcp/fcc	−3.298/−3.240	1.13/1.09	
OH	fcc/hcp	−5.627/−5.541	1.32/1.33	0.98/0.98

Table 3
Calculated structural parameters, adsorption energy for the final H + OH configurations and the dissociation barriers of water molecule on Zr(0001) surface. E_d (eV) represents the dissociation barrier. $Site_H$ and $Site_{OH}$ represent the positions of H and OH species in the dissociative configuration, respectively.

Path	E_a	E_d	Φ	$Site_H$	$Site_{OH}$	z_H	z_O	d_{O-H}
top-x	−2.905	0.106	3.16	fcc	hcp	1.07	1.34	0.97
top-$y1$	−2.905	0.261	3.16	fcc	hcp	1.07	1.34	0.97
top-$y2$	−2.730	0.371	3.18	hcp	fcc	1.09	1.38	0.97
bri-z	−2.905	0.093	3.16	fcc	hcp	1.07	1.34	0.97

3.2. Diffusion of H_2O molecule

Given a H_2O molecule at a stable adsorption site, it is interesting to see how it diffuses on the substrate. Here, therefore, we calculate the diffusion paths and energetic barriers of water on Zr(0001) surface between neighboring adsorption sites along the top-x, top-$y1$ and top-$y2$ channels respectively, which are schematically shown in the insets of Fig. 4. Each lateral diffusion path adopted here connects two minimum energy states on the top sites, through the bridge site as a transition state. The adsorption energies as a function of the lateral displacement of O atom are shown in Fig. 4.

For the channel top-$y1$, the transition state with the energy maximum located on the bridge site, which is not a stable adsorption site. It is found that the water molecule moves towards the adjacent top-$y1$ site straightforwardly, with slight wiggling along the diffusion path. Moreover, the diffusion energy barrier 0.315 eV along this path is much lower than the adsorption energy on top-$y1$ site, implying that the water molecule has a high mobility on the Zr(0001) surface. This is the same trend that is found for the channel top-$y2$, with a lower barrier 0.280 eV.

In the case of channel top-x, the lower diffusion barrier 0.061 eV indicates a higher mobility than that along those fore-mentioned two channels. Furthermore, there exists a local energy minimum along this diffusion path. Investigation in more detail in this particular case reveals that this energy minimum coincides with the stable bridge adsorption site bri-z, which means that the water molecule may rotate during the diffusion. We find that as the water molecule migrates towards the adjacent top site, it rotates around the O atom and overcomes an energy barrier, till the tilt angle reaches as high as 71°, where the molecule moves to the bridge site as a transition state. Then the water molecule rotates reversely, overcoming another barrier and arriving at the adjacent top-x site. This energy minimum state located on the bridge site may also give a reason why this channel possesses the lowest diffusion barrier.

The energy barriers of these lateral diffusion channels are larger than that of the azimuthal rotations mentioned above. While the Arrhenius-type activation process $k = Ae^{-\varepsilon/k_BT}$ can be adopted here, where A is the prefactor here equal to the attempt frequency, k_B is the Boltzmann constant, and ε is the energy barrier. By assuming the attempt frequency 10^{13} Hz of the adsorbate and setting the rate constant k equal to 1, the energy barriers of these three diffusion

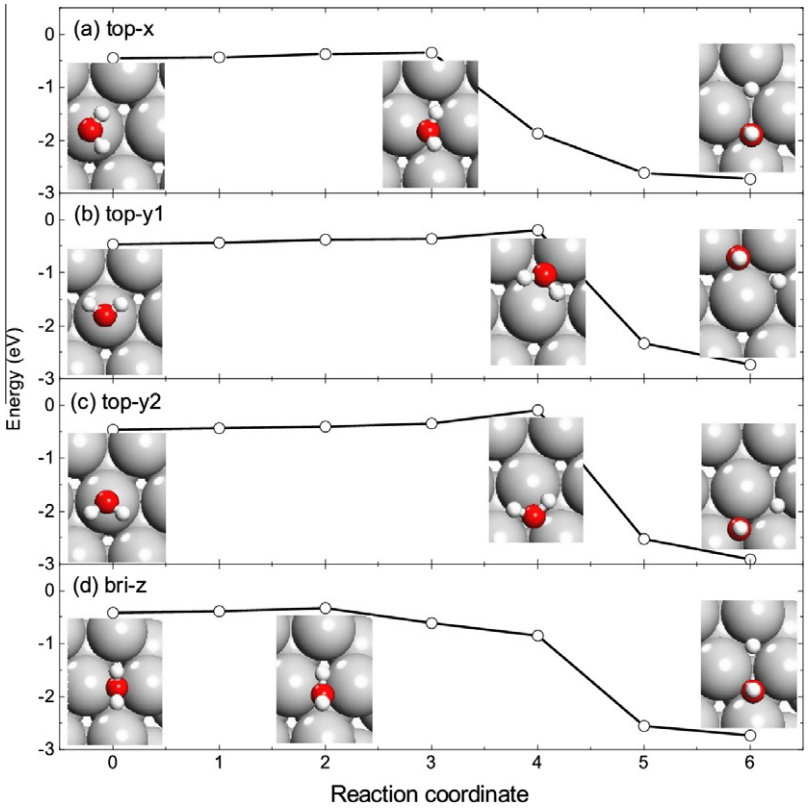

Fig. 5. Four water dissociation paths considered in this study, corresponding to the four most stable adsorption states represented in Fig. 1. The inset pictures show the structures of H_2O/Zr(0001) surface corresponding to the adsorption, transition and dissociation states, respectively.

channels top-x, top-$y1$ and top-$y2$ correspond to temperature of about 24, 122, and 109 K, respectively, suggesting that the diffusion can occur under room temperature on the H_2O/Zr(0001) surface, especially for the channel top-x. These results provide evidence that the water molecules are very mobile on Zr(0001), even at very low temperature [29].

3.3. Dissociation of H_2O molecule

In order to investigate the water dissociation process, we begin with the adsorption properties of the dissociated H and OH species. The structural and energetic details of these species are summarized in Table 2. For the H species, the hcp site is the most stable with an adsorption energy of −3.298 eV, and the fcc site is slightly less stable with an adsorption energy of −3.240 eV. Next, for the OH species, the most stable site is found to be fcc with an adsorption energy of −5.627 eV, and the hcp site is less stable by 0.086 eV than the fcc site. The O–H bond length (0.98 Å) with O atom end-on orientation is less than that (1.00 Å) of the free OH molecule.

We examine four probable dissociation paths of H_2O molecule on the Zr(0001) surface. The initial states as the precursors for dissociation are four stable molecular adsorption states discussed above. For the final states, based on the results of the adsorption of H and OH, we consider several possible combinations of the adsorption sites for H and OH species. It is found that for the H + OH configuration, the H and OH species occupy two neighboring hollow sites (fcc and hcp) respectively connected via a bridge site, which is the most stable. Table 3 shows the structural and energetic details of the final H + OH configurations. With low adsorption energies and work functions, these two species strongly bond to the surface, The O–H bond orients almost perpendicular to the surface, and the bond length 0.97 Å differs only slightly from that of the adsorbed H_2O molecule.

Fig. 5 shows the energy profiles for these dissociation paths. The activation energies for the dissociation of the water molecules are 0.093, 0.106, 0.261 and 0.371 eV along the paths bri-z, top-x, top-$y1$ and top-$y2$, respectively (see Table 3). We find that the paths top-x and bri-z have noticeably low dissociation barriers, small enough to facilitate the dissociations of the adsorbed water molecules. While for the paths top-$y1$ and top-$y2$, the energy barriers are higher than that of the forenamed two paths. The reason why such differences exist about the energy barriers will be clear when we go deep into the dissociation process. For the path bri-z, it can be seen (from the inset pictures of Fig. 5) that the water molecule starts to dissociate almost *in situ*, hence the energy barrier is low. In the case of path top-x, the water molecule first migrates to the adjacent bridge site, meanwhile the molecule rotates around the O atom for a larger tilt angle (which it can do with little energy loss), then following the dissociation process just as in the path bri-z. On the other hand, for the dissociation paths top-$y1$ and top-$y2$, before reaching the transition states, the water molecules have to rotate more complexly, then enter the dissociation process with the H and OH species moving to their final positions.

Within the same Arrhenius-type activation process used above, the energy barriers of these four dissociation paths correspond to temperature of about 36, 41, 101 and 144 K, respectively, suggesting that the dissociation can occur under room temperature on the H_2O/Zr(0001) surface, especially for the path bri-z. This is in good accordance with the experimental observations that water can dissociate on the Zr(0001) surface [16,17], but different from the dissociation of water on other transition metal surfaces such as Fe(100) [6], Rh(111) and Ni(111) [30], which need to overcome much higher barriers.

4. Conclusions

We have systematically studied the adsorption and dissociation behaviors of H_2O on Zr(0001) surface by using first-principles DFT method. We found that there exist two kinds of adsorption structures with almost the same adsorption energy as the locally stable states, including flat and upright configurations respectively. It was found that dominated by the $1b_1$–d band coupling, the flat adsorption states on the top site are insensitive to the azimuthal orientation. The diffusion between adjacent top sites reveals high mobility of the water molecule on Zr(0001). For the upright configuration, we have found that the hybridization between the d band of the Zr(0001) surface and MOs $1b_1$ and $3a_1$ of the water, as well as the charge transfer between the adsorbate and the substrate, contribute to the adsorption system. Consistent with previous experimental results, the dissociation of H_2O has been found to be very facile, especially for the upright configuration. It must be noted that the current discussion of diffusion process is based on perfect stoichiometric surface, and the prospects could be much different on a natural rough surface. Nevertheless, we expect that the present results are helpful for the practical usage of zirconium in nuclear reactors.

References

[1] P.A. Thiel, T.E. Madey, Surf. Sci. Rep. 7 (1987) 211.
[2] M.A. Henderson, Surf. Sci. Rep. 46 (2002) 1.
[3] R. Brosseau, M.R. Brustein, T.H. Ellis, Surf. Sci. 294 (1993) 143.
[4] S. Wang, Y. Cao, P.A. Rikvold, Phys. Rev. B 70 (2004) 205410.
[5] W.-H. Hung, J. Schwartz, S.L. Bernasek, Surf. Sci. 248 (1991) 332.
[6] S.C. Jung, M.H. Kang, Phys. Rev. B 81 (2010) 115460.
[7] K.G. Lloyd, B.A. Banse, J.C. Hemminger, Phys. Rev. B 33 (1986) R2858.
[8] J. Li, S. Zhu, Y. Li, F. Wang, Phys. Rev. B 76 (2007) 235433.
[9] S. Seong, A.B. Anderson, J. Phys. Chem. 100 (1996) 11744.
[10] K. Morgenstern, K.H. Rieder, J. Chem. Phys. 116 (2002) 5746.
[11] A. Michaelides, V.A. Ranea, P.L. de Andres, D.A. King, Phys. Rev. Lett. 90 (2003) 216102.
[12] S. Meng, E.G. Wang, S. Gao, Phys. Rev. B 69 (2004) 195404.
[13] J. Carrasco, A. Michaelides, M. Scheffler, J. Chem. Phys. 130 (2009) 184707.
[14] N. Stojilovic, E.T. Bender, R.D. Ramsier, Prog. Surf. Sci. 78 (2005) 101.
[15] B. Li, K. Griffiths, C.-S. Zhang, P.R. Norton, Surf. Sci. 370 (1997) 97.
[16] B. Li, K. Griffiths, C.-S. Zhang, P.R. Norton, Surf. Sci. 384 (1997) 70.
[17] V. Dudr, F.S. utara, T. Skála, M. Vondráček, N. Tsud, V. Matolín, K.C. Prince, V. Cháb, Surf. Sci. 600 (2006) 3581.
[18] G. Kresse, J. Furthmuller, Phys. Rev. B 54 (1996) 11169.
[19] J.P. Perdew, K. Burke, M. Ernzerhof, Phys. Rev. Lett. 77 (1996) 3865.
[20] G. Kresse, D. Joubert, Phys. Rev. B 59 (1999) 1758.
[21] L. Bengtsson, Phys. Rev. B 59 (1999) 12301.
[22] H.J. Monkhorst, J.D. Pack, Phys. Rev. B 13 (1976) 5188.
[23] M. Weinert, J.W. Davenport, Phys. Rev. B 45 (1992) 13709.
[24] S.-X. Wang, P. Zhang, P. Zhang, J. Zhao, S.-S. Li, Phys. Lett. A 375 (2011) 3208.
[25] H. Jónsson, G. Mills, K.W. Jacobsen, in: B.J. Berne et al. (Eds.), Classical and Quantum Dynamics in Condensed Phase Simulations, World Scientific, Singapore, 1998.
[26] D. Eisenberg, W. Kauzmann, The Structure and Properties of Water, Oxford University Press, New York, 1969.
[27] Y.S. Zhao, J.Z. Zhang, C. Pantea, J. Qian, L.L. Daemen, P.A. Rigg, R.S. Hixson, G.T. Gray III, Y.P. Yang, L.P. Wang, T.Y. Uchida, Phys. Rev. B 71 (2005) 184119.
[28] G. Blyholder, J. Phys. Chem. 68 (1964) 2772.
[29] T. Mitsui, M.K. Rose, E. Fomin, D.F. Ogletree, M. Salmeron, Science 297 (2002) 1850.
[30] M. Pozzo, G. Carlini, R. Rosei, D. Alfè, J. Chem. Phys. 126 (2007) 164706.